




Viral Inactivation Impacts Microbiome Estimates in a Tissue-Specific Manner

 Alba Boix-Amorós,^{a,b} Enrica Piras,^{a,b} Kevin Bu,^a David Wallach,^a Matthew Stapylton,^a Ana Fernández-Sesma,^c Dolores Malaspina,^{a,d} Jose C. Clemente^{a,b}

^aDepartment of Genetics and Genomic Sciences, Icahn School of Medicine at Mount Sinai, New York, New York, USA

^bPrecision Immunology Institute, Icahn School of Medicine at Mount Sinai, New York, New York, USA

^cDepartment of Microbiology, Icahn School of Medicine at Mount Sinai, New York, New York, USA

^dDepartment of Neuroscience, Icahn School of Medicine at Mount Sinai, New York, New York, USA

ABSTRACT The global emergence of novel pathogenic viruses presents an important challenge for research, as high biosafety levels are required to process samples. While inactivation of infectious agents facilitates the use of less stringent safety conditions, its effect on other biological entities of interest present in the sample is generally unknown. Here, we analyzed the effect of five inactivation methods (heat, ethanol, formaldehyde, psoralen, and TRIZOL) on microbiome composition and diversity in samples collected from four different body sites (gut, nasal, oral, and skin) and compared them against untreated samples from the same tissues. We performed 16S rRNA gene sequencing and estimated abundance and diversity of bacterial taxa present in all samples. Nasal and skin samples were the most affected by inactivation, with ethanol and TRIZOL inducing the largest changes in composition, and heat, formaldehyde, TRIZOL, and psoralen inducing the largest changes in diversity. Oral and stool microbiomes were more robust to inactivation, with no significant changes in diversity and only moderate changes in composition. *Firmicutes* was the taxonomic group least affected by inactivation, while *Bacteroidetes* had a notable enrichment in nasal samples and moderate enrichment in fecal and oral samples. *Actinobacteria* were more notably depleted in fecal and skin samples, and *Proteobacteria* exhibited a more variable behavior depending on sample type and inactivation method. Overall, our results demonstrate that inactivation methods can alter the microbiome in a tissue-specific manner and that careful consideration should be given to the choice of method based on the sample type under study.

IMPORTANCE Understanding how viral infections impact and are modulated by the microbiome is an important problem in basic research but is also of high clinical relevance under the current pandemic. To facilitate the study of interactions between microbial communities and pathogenic viruses under safe conditions, the infectious agent is generally inactivated prior to processing samples. The effect of this inactivation process in the microbiome is, however, unknown. Further, it is unclear whether biases introduced by inactivation methods are dependent on the sample type under study. Estimating the magnitude and nature of the changes induced by different methods in samples collected from various body sites thus provides important information for current and future studies that require inactivation of pathogenic agents.

KEYWORDS 16S RNA, DNA sequencing, human microbiome, viral inactivation

A homeostatic microbiome is essential at the physiological, immunological, and metabolic levels for human health, and alterations in its composition have been linked to several diseases, ranging from intestinal inflammatory conditions (1–3) to respiratory infections (4, 5), asthma and allergies (6–8), or even neurological disorders (9–11).

Citation Boix-Amorós A, Piras E, Bu K, Wallach D, Stapylton M, Fernández-Sesma A, Malaspina D, Clemente JC. 2021. Viral inactivation impacts microbiome estimates in a tissue-specific manner. *mSystems* 6:e00674-21. <https://doi.org/10.1128/mSystems.00674-21>.

Editor Ileana M. Cristea, Princeton University

Copyright © 2021 Boix-Amorós et al. This is an open-access article distributed under the terms of the [Creative Commons Attribution 4.0 International license](https://creativecommons.org/licenses/by/4.0/).

Address correspondence to Jose C. Clemente, jose.clemente@mssm.edu.

Received 2 June 2021

Accepted 8 September 2021

Published 5 October 2021

Furthermore, growing evidence suggests that alterations in the human microbiome may also occur in response to viral infections (12–17). Bacteria can also play important roles during viral infection processes, ranging from offering protection against viral agents (18–22) to facilitating viral infections or participating in bacterial-viral coinfections (23–27). The continuous emergence of novel pathogenic viruses at a global scale, such as the H1N1 influenza A virus (28, 29), or the coronaviruses responsible for the severe acute respiratory syndrome (SARS-CoV) (30, 31), the Middle East respiratory syndrome (MERS-CoV) (32, 33), or the more recent SARS-CoV-2 causative of the current COVID-19 pandemic (34, 35), emphasizes the need to understand how microbial communities might be related to these pathogens and whether they modulate infection risk.

Working with highly infectious viral agents requires biosafety level 3 (BSL3) or 4 (BSL4) containment laboratories, which poses significant challenges for most researchers. Biosafety labs are generally limited to specialized research centers or hospitals and often cannot accommodate specific equipment, such as flow cytometers or microscopes, which are required for analyses. Viral inactivation methods allow the removal of highly infectious agents and facilitate the processing of samples in lower-level biosafety conditions following appropriate safety practices (28, 36, 37), thus expanding the analyses that can be performed on such samples. The 2019 SARS-CoV-2 pandemic, for example, has resulted in a widespread interest for researchers to study clinical samples from subjects with known or suspected COVID-19. These studies often require the use of effective viral inactivation methods that allow the manipulation of samples in different biosafety research environments. Several methods have been shown to effectively inactivate SARS-CoV-2 and have permitted the study of the virus in laboratories of different scientific backgrounds in an unprecedented global effort to unravel the virus pathogenesis and end the pandemic (38–41). Previous studies have shown that sample storage methods and, in particular, different temperatures, freeze-thaw cycles, and DNA preserving reagents, can impact microbial communities' composition and stability (42–48) and that some microbial inactivation methods differentially preserve microbial nucleotides for subsequent PCR or immunoassay analysis (39, 44, 49). However, there is currently no evidence on the effect of viral inactivation methods in microbial composition and structure, which potentially represents a major source of biases in studies characterizing the microbiome of infected subjects (12, 16, 17, 50–53). It is therefore fundamental to quantify the effect of viral inactivation methods on different sample types to ensure the robustness of conclusions.

Here, we compared microbiome composition and diversity, as inferred from 16S rRNA amplicon sequencing, after treating samples representative of four different body sites (oral, nasal, skin, and stool) with five commonly used viral inactivation methods or reagents (heat killing at 56°C for 30 min, 75% ethanol, psoralen, 4% formaldehyde, and TRIzol) and compared them with untreated samples. Our results thus aim to identify inactivation methods that ensure the preservation of microbial communities across different body sites.

RESULTS

Microbial community composition is impacted by viral inactivation protocols.

To assess differences in bacterial community structure, we performed principal coordinate analysis (PCoA) based on weighted UniFrac distances. In the absence of inactivation ("no treatment"), samples clustered by body site (Kruskal-Wallis, $P < 0.001$) (Fig. S1 in the supplemental material), with dispersion of samples (variances) also differing significantly across body sites (permutation test, $P < 0.001$), as previously reported (54). Stool and oral samples separated along the first principal coordinate, while nasal and skin samples were more scattered on the plot, indicative of a more variable microbiome composition. While samples separated primarily by body site, there were also significant changes associated with different inactivation protocols (Fig. 1A). These observations were confirmed by a distance-based permutational multivariate analysis of variance (adonis), which showed that body site and inactivation were both

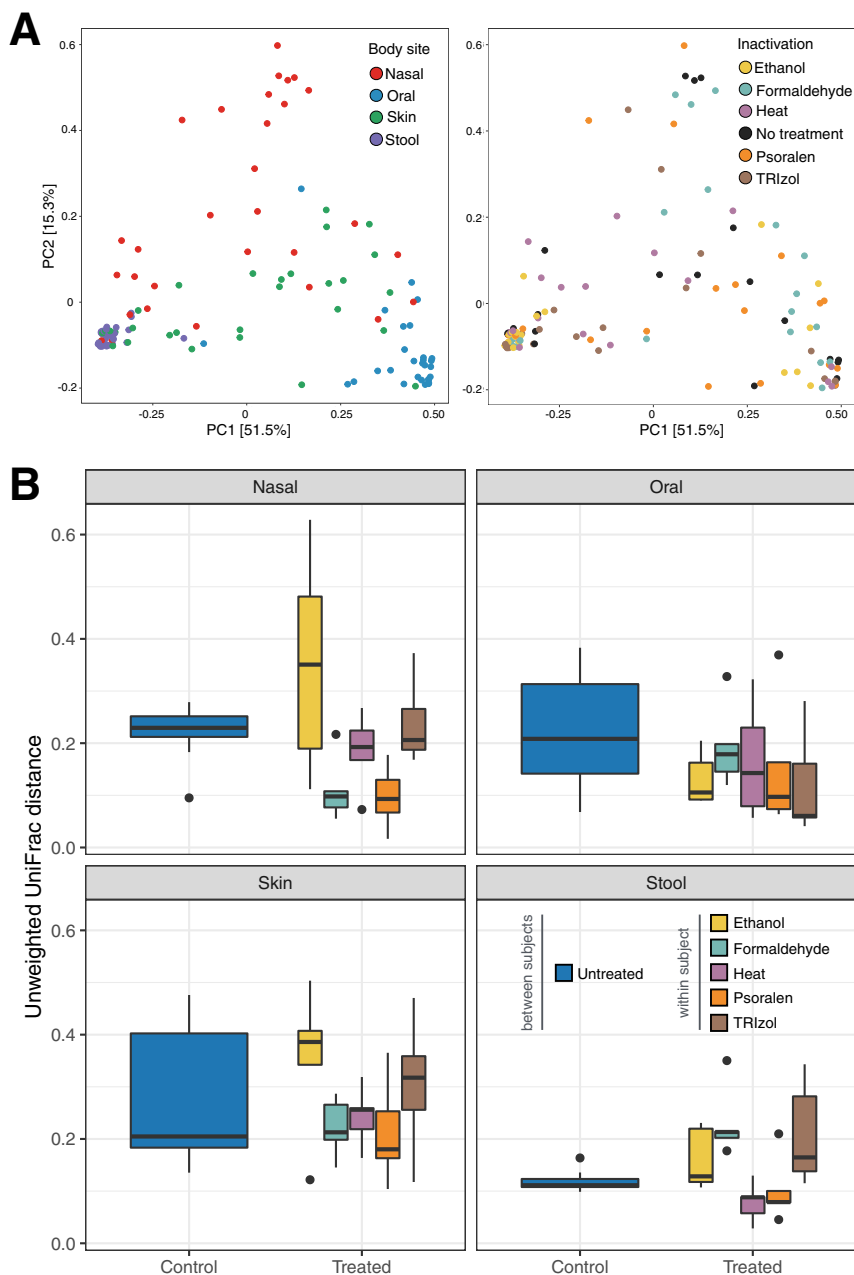


FIG 1 Impact of body site and inactivation treatments in microbiome composition. (A) PCoA plots based on weighted UniFrac distances, with samples colored by body site (left) and inactivation protocol (right). (B) Weighted UniFrac distances between untreated samples from different subjects and between untreated and inactivated samples from the same subjects for each inactivation method and body site.

significantly associated with composition ($P = 0.001$), although body site explained a larger percentage of the total variability in the data set (43% versus 7%).

We next tested whether inactivation methods introduce changes in microbiome structure of less magnitude than those observed between untreated samples of different subjects. For each body site, we compared the distribution of UniFrac distances in untreated samples of different subjects (i.e., the intersubject distances) against the distribution of distances between the untreated and inactivated samples of each subject (the intrasubject distances) for each inactivation method (Fig. 1B). While the degree of change varied per body site and method, all inactivation protocols resulted in

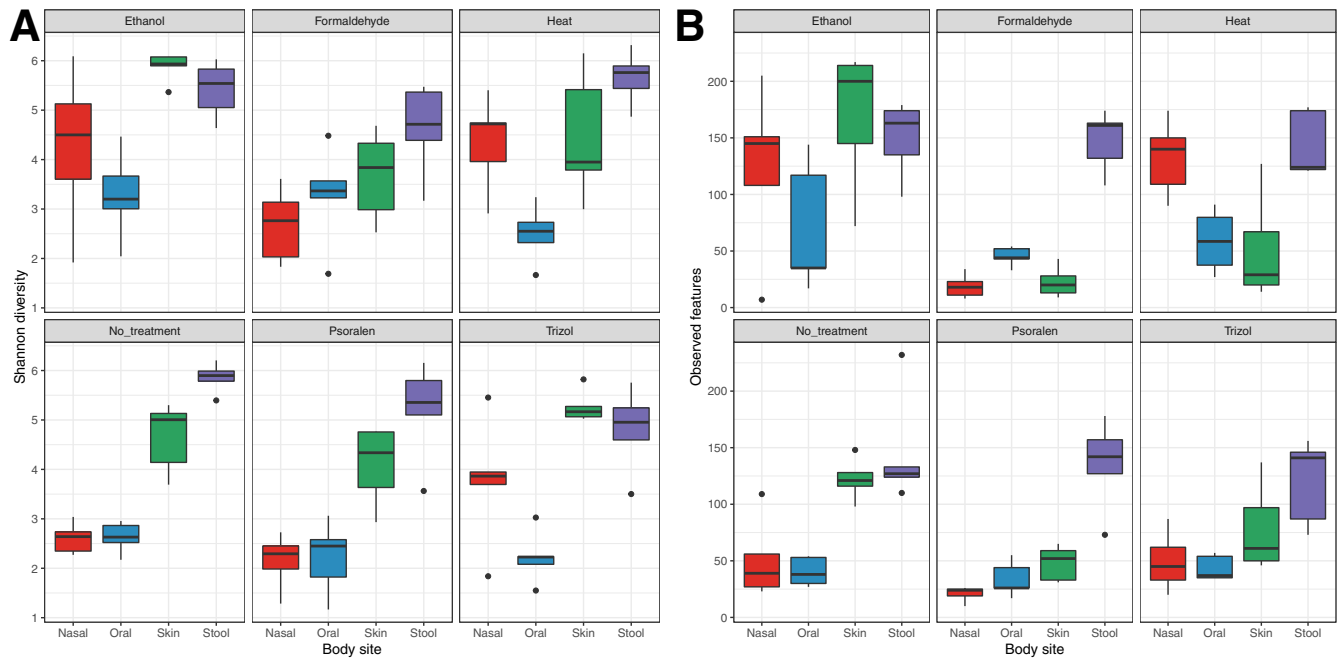


FIG 2 Microbial alpha diversity across inactivation treatments. (A) Observed number of features per inactivation method and body site. (B) Shannon diversity indices per inactivation method and body site. Samples appear colored by body site.

distances from the untreated sample that were not significantly different than those observed between untreated samples of different subjects (analysis of variance [ANOVA], $P > 0.05$). Oral and stool samples were, in general, the least affected by inactivation, while psoralen was the protocol that most consistently conserved the microbiome structure of the samples. Ethanol introduced particularly large changes in nasal and skin samples, while TRIZol disrupted more noticeably the microbiome of skin and stool samples. Overall, these results demonstrate that inactivation methods introduce notable changes to the microbiome across all body sites, of similar magnitude to those observed when comparing the microbial communities of different subjects.

Viral inactivation induces shifts in alpha diversity. Microbial alpha diversity also varied across body sites, as observed in the nontreated samples (Kruskal-Wallis, observed features, $P = 0.003$; Shannon, $P = 0.001$). Both the number of observed features and Shannon indices varied significantly across body sites (Kruskal-Wallis, $P = 1.1E^{-8}$ and $P = 5.3E^{-13}$, respectively) and inactivation treatments ($P = 0.002$; $P = 0.039$) (Fig. S2). We further used generalized linear models to study the effect of inactivation treatments in alpha diversity when controlling for sample type and subject. Formaldehyde treatment reduced Shannon diversity in skin and stool samples ($P = 0.02$ and $P = 0.01$, respectively), while heat and TRIZol increased the diversity of nasal samples ($P = 0.01$; $P = 0.03$) (Fig. 2A). On the other hand, formaldehyde, heat, and psoralen treatments resulted in a decrease in the observed number of features in skin samples ($P = 0.001$, $P = 0.008$, and $P = 0.03$, respectively), while heat inactivation of nasal samples resulted in an increase in the observed features ($P = 0.046$) (Fig. 2B).

Changes in taxonomic profiles after inactivation. We next evaluated the effect of the inactivation methods on the taxonomic profiles of each sample type (Fig. S3). At the phylum level, stool samples were dominated by *Firmicutes* (mean \pm standard deviation [SD], 70% \pm 20%) and *Bacteroidetes* (25% \pm 17%). Oral samples were dominated by *Firmicutes* (61% \pm 24%) and *Proteobacteria* (30% \pm 23%), and nasal and skin samples were dominated by *Firmicutes* (45% \pm 18% and 65% \pm 16%, respectively), *Actinobacteria* (38% \pm 23% and 14% \pm 11%, respectively) and *Proteobacteria* (11% \pm 14% and 11% \pm 13%, respectively). Taxonomic composition was differentially affected by inactivation treatment, depending on sample type (Fig. 3). While oral samples were generally stable



FIG 3 Enrichment and depletion across body sites and inactivation treatments for major bacterial phyla. Barplots represent the \log_2 fold change in bacterial relative abundances at the phylum level between each inactivation treatment and no treatment. Fold changes with positive values represent an increase in relative abundance after inactivation, while negative values indicate reduced relative abundances.

and did not exhibit major changes with any method, all other sample types were impacted by the inactivation process. Across all samples, *Firmicutes* was the phylum least affected by inactivation treatments, while the effect on the other phyla varied in magnitude depending on the sample type. Stool samples were depleted of *Actinobacteria*, while abundances of *Proteobacteria* and, to a lesser extent, *Bacteroidetes*, were enriched across inactivation treatments. In this sample type, heat and psoralen introduced only small amounts of change. On the other hand, inactivation treatments led to a notable enrichment of *Bacteroidetes* in the nasal samples, particularly with ethanol. Other phyla were generally robust to inactivation treatments except the *Proteobacteria*, which was depleted by psoralen in these samples. Skin samples were mostly affected by ethanol and TRIZOL, which depleted *Actinobacteria* and *Proteobacteria*, with moderate enrichment of the *Proteobacteria* (psoralen, formaldehyde) and the *Bacteroidetes* (ethanol, TRIZOL, heat).

Differential enrichment analysis identifies tissue-specific effects of inactivation.

We further analyzed the effect of inactivation in microbial composition using differential enrichment analysis (55) to identify specific taxa that were significantly enriched or depleted at each body site and for each inactivation method (Fig. 4).

Overall, inactivation with ethanol and formaldehyde introduced the highest variability, as linear discriminant analysis effect size (LEfSe) analysis identified multiple differential taxa across all four body sites (Fig. S4). Across body sites, ethanol and formaldehyde induced changes in all sample types. TRIZOL also introduced compositional differences in all sample types except for oral. Inactivation with heat resulted in moderate changes that were tissue dependent, and psoralen induced only a minimal reduction of bacterial abundances in the inactivated samples compared to no treatment (Fig. 4).

Skin and nasal samples had the highest number of differentially abundant taxa after inactivation. Skin samples were particularly sensitive to ethanol, as shown by a higher logarithmic discriminant analysis (LDA) effect size and a larger number of differentially

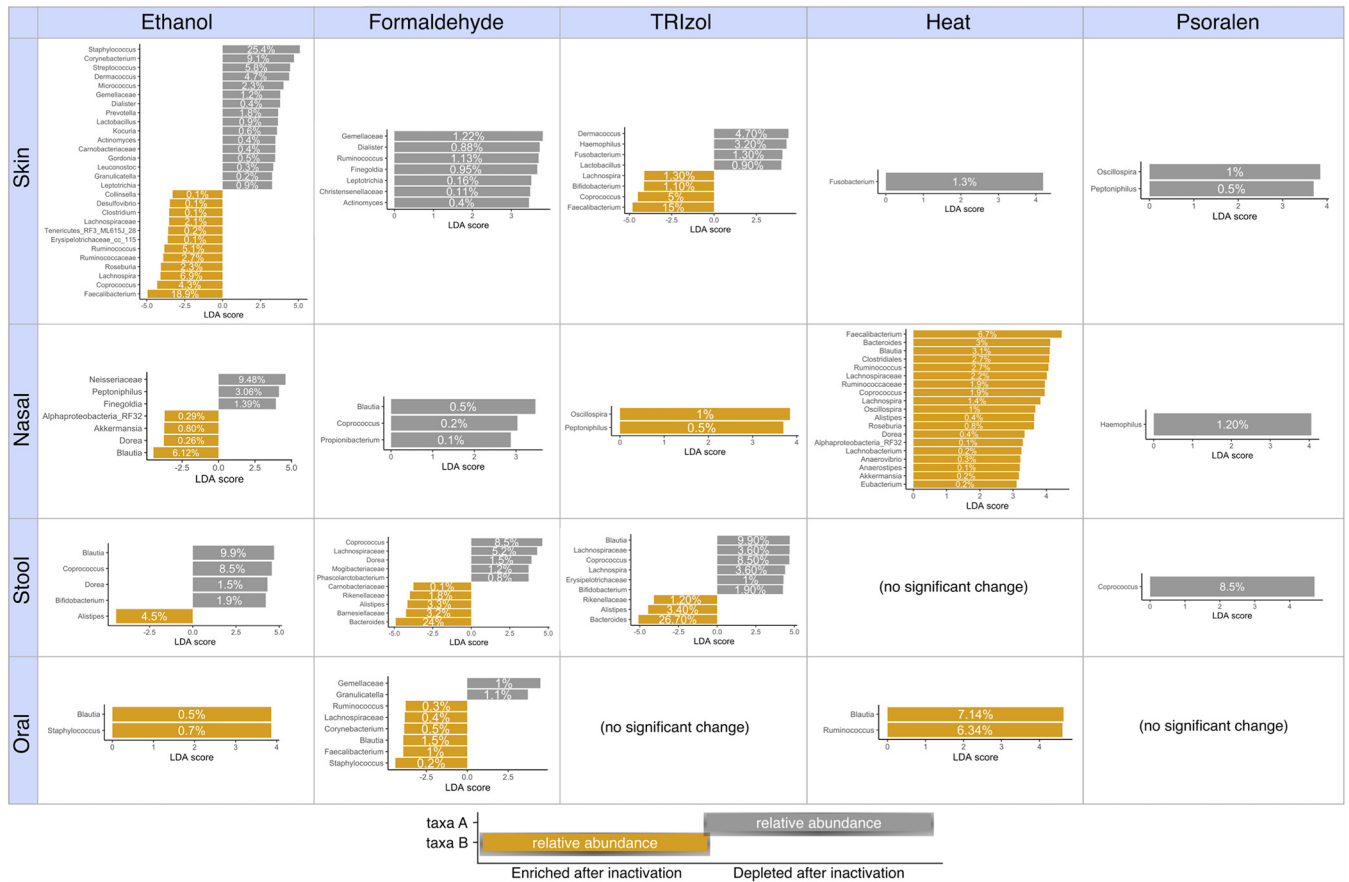


FIG 4 Bacterial taxa associated with viral inactivation treatments across body sites. Differentially abundant taxa enriched or depleted with each inactivation treatment and for each body site, as inferred by the LEfSe algorithm for biomarker discovery. The threshold for logarithmic discriminant analysis (LDA) score was 2, and significance was a *P* value of <0.05.

abundant genera. TRIZOL also increased the abundance of several taxa, including *Faecalibacterium*, *Coprococcus*, and *Lachnospira*, while some common skin microbes, such as *Staphylococcus*, *Corynebacterium*, and *Dermacoccus*, were depleted. Compared to formaldehyde, heat, and psoralen treatments, untreated skin samples also showed an enrichment of other low-abundance bacteria, including *Gemellaceae*, *Ruminococcus*, and *Fusobacterium*. Nasal samples were mostly affected by ethanol, TRIZOL, and heat treatments, which resulted in an enrichment of *Blautia*, *Ruminococcus*, *Faecalibacterium*, and *Bacteroides*, among others. Ethanol also depleted *Neisseriaceae* and *Peptoniphilus*. In stool samples, ethanol enriched the genus *Alistipes*, while formaldehyde and TRIZOL enriched mostly *Bacteroides*. On the other hand, all three treatments reduced the abundance of different fecal microorganisms, including *Blautia*, *Coprococcus*, and *Lachnospiraceae*, among others. Psoralen and heat preserved microbial communities in stool samples more robustly, with only *Coprococcus* being impacted by psoralen. Finally, oral samples showed the least number of taxa differentially enriched after inactivation. Formaldehyde treatment reduced the abundance of *Gemellaceae* and *Granulicatella* and increased the abundance of *Blautia* and *Faecalibacterium* (among others). Heat increased the abundance of *Blautia* and *Ruminococcus*, while TRIZOL and psoralen treatments did not affect oral composition significantly.

To account for potential associations between viral inactivation methods and enrichment in bacterial contaminants commonly found in kits and other laboratory reagents, we compared the abundance of contaminant taxa (Table S1) across inactivation methods. Analysis of composition of microbiomes (ANCOM) (56) identified one family, *Bradyrhizobiaceae*, that was enriched in formaldehyde, heat, and TRIZOL treatments (*W* = 67) (Fig. S5).

TABLE 1 Summary of the effects of inactivation methods in microbial diversity estimates and taxonomy^a

Body site	Major findings					Suggested inactivation					
	Beta diversity	Alpha diversity (obs. feats / Shannon)		Taxonomy							
				FA	EtOH		Heat	Pso	TRI		
Nasal	↑ EtOH	Obs. features	↑ Heat		Actino						FA Psoralen
		Shannon	↑ Heat ↑ TRlzol		Bact	Bright green				Bright green	
				Firmi							
				Proteo					Bright red		
Oral	(no sig. change)	Obs. features	(no sig. change)		Actino	Pale green					EtOH FA Heat Psoralen TRlzol
		Shannon	(no sig. change)		Bact						
				Firmi							
				Proteo							
Skin	↑ EtOH ↑ TRlzol	Obs. features	↓ FA ↓ Heat ↓ Psoralen		Actino		Bright red			Bright red	Psoralen
		Shannon	↓ FA		Bact						
				Firmi							
				Proteo		Bright red				Bright red	
Stool	↑ TRlzol	Obs. features	(no sig. change)		Actino	Bright red				Bright red	Psoralen Heat
		Shannon	↓ FA		Bact	Pale green				Pale green	
				Firmi							
				Proteo		Bright green	Pale green				

^aBright green, high enrichment; pale green, moderate enrichment; pale red, moderate depletion; bright red, high depletion.

DISCUSSION

Highly pathogenic viruses can only be handled in biocontainment BSL3 or BSL4 laboratories and must be rendered noninfectious before samples can be manipulated at lower biosafety levels. In this study, we aimed to quantify the effect of five commonly used inactivation methods (heat, ethanol, psoralen, TRlzol, and formaldehyde) in the microbiomes of samples collected from four human body sites. Because each individual harbors a unique microbiome (57, 58), inactivation methods that introduce changes lower than those observed between different subjects are desirable. By comparing the effect of these methods versus untreated samples, we estimated the magnitude of change introduced by each inactivation protocol and identified their biases across body sites. Overall, every method introduced compositional and diversity changes that differed across tissues (Table 1). Skin samples were the most impacted by inactivation and exhibited the highest levels of dispersion, followed by nasal samples. Oral samples, on the other hand, were mostly stable regardless of treatment, showing only minor differences compared to untreated samples. Despite having the lowest microbiome variability among the body sites under study, stool samples were also impacted by inactivation, particularly in the abundance of specific bacterial phyla. *Firmicutes* consistently had the smallest amount of change across inactivation methods. *Bacteroidetes* suffered minor changes in skin and oral samples, moderate in fecal, and high in nasal samples. *Actinobacteria* were highly depleted in fecal and skin samples (particularly with ethanol and TRlzol in the latter), moderately depleted in oral samples treated with ethanol or TRlzol, and mostly unchanged in nasal samples. Finally, *Proteobacteria* were highly impacted in fecal samples, highly depleted in nasal samples treated with psoralen, and highly depleted in skin samples treated with ethanol and TRlzol.

Ethanol treatment introduced the largest amount of change across sample types. Alcohols can effectively inactivate a wide spectrum of bacteria, fungi, and viruses by disrupting cell membranes and denaturing proteins (59–61). At the same time,

alcohols' fixative properties preserve viral and bacterial structures and safely allow further downstream analysis (61–63). For this reason, ethanol has been commonly used as preserving agent in microbiome samples (64–66). Due to its low cost and accessibility, ethanol is an attractive option for viral inactivation. However, and to the best of our knowledge, the effect of inactivation using ethanol on microbiome composition and diversity has not been evaluated previously. Here, we used a 75% ethanol formulation (67–69) and found that the stability of bacterial communities was generally compromised by this treatment, particularly in skin and nasal samples. In skin samples, important commensals such as *Staphylococcus* or *Corynebacterium* were greatly depleted after ethanol treatment, while we observed an enrichment in bacteria such as *Faecalibacterium*, *Lachnospira*, or *Coprococcus*. In nasal samples, *Neisseriaceae* relative abundance was reduced, while that of *Blautia* increased. Ethanol inactivation resulted in moderate changes in stool samples and only introduced small changes in oral samples, in both cases affecting mostly bacterial taxa present at low abundance. The virucidal properties of ethanol are optimal when used at 60% to 80% concentration, as water facilitates protein denaturation (59, 70, 71). However, previous studies have shown that preserving microbiome samples with 70% ethanol can have detrimental effects on DNA yields, resulting in lower concentrations than freezing or other preservation methods (43, 65, 66).

TRIzol also introduced important changes in the microbiome of different body sites, particularly skin and stool. TRIzol is a widely used lysing solution that has been classically used for the cellular extraction of nucleic acids and proteins. The combined effect of phenol and guanidine isothiocyanate components of TRIzol disrupts cell membranes and denatures proteins, making this reagent effective at inactivating viruses (49, 72–74). Buffers containing TRIzol are commonly used for sample storage, as TRIzol also denatures DNase and RNase enzymes, thus protecting DNA and RNA from degradation (75). However, in our study, TRIzol treatment had important effects across samples from different body sites. Skin samples were especially affected by TRIzol, and, as we observed with ethanol, biases were notable in a wide variety of taxa. Stool and nasal samples had only moderate changes, while oral samples seemed to be robust to this treatment. In a recent study, incubation of samples containing SARS-CoV-2 with 10% TRIzol for 10 min was shown to reduce the levels of viral RNA detection by digital PCR (38). Further, it has been previously shown that microbiome samples stored in TRIzol had lower diversity than storage in phosphate-buffered saline (PBS), suggesting that this reagent may deplete part of the nucleic acids in the samples and thus may not be suitable for microbiome studies (75).

Formaldehyde resulted in a more heterogeneous set of results in our study. Formaldehyde is a fixative agent that is ubiquitously used in laboratory settings, including analysis of infected cells or microbial preparations for microscopy or flow cytometry. By cross-linking proteins, formaldehyde is able to inactivate cells while preserving their structural form, and it has been widely used in various concentrations for the inactivation of viruses (49, 73, 76–79). However, this reagent alters cellular structures and can render samples unusable for some molecular and/or immunological downstream analysis (80, 81). While nasal samples seemed to suffer only minimal effects, formaldehyde introduced moderate changes in oral, skin, and stool samples. Previous reports have shown partial bacterial, fungal, and viral inactivation with formaldehyde, likely due to inherent differences in microbial cell walls composition, i.e., peptidoglycan thickness (82–85). Therefore, it is possible that the effects of this reagent on the microbiome may differ depending on the precise bacteria composing each sample type.

Inactivation with psoralen had the least effect on microbial communities across body sites. Psoralen is a photoreactive, small compound of natural origin that has a wide range of pharmacologic applications. Psoralen can cross phospholipid bilayers and intercalate into nucleic acids and, upon exposure to UV (UV-A) radiation (PUVA), causes interstrand cross-linking and impedes replication. Psoralen effectively

inactivates pathogens, including viral agents, while preserving structures and nucleic acids that allow for further antigenic and genomic analyses to be performed (37, 86–89). In our results, psoralen generally resulted in minimal changes compared to other inactivation treatments. Although PUVA is a common phototherapy used to treat various skin disorders, such as psoriasis or dermatitis (90, 91), we found no previous reference to how it might affect microbiome composition and diversity. The main drawback of using psoralen is its higher cost, being the most expensive among all the inactivation methods tested in this study.

The effect of heat, an affordable and broadly used method to inactivate highly pathogenic organisms, was also tested. By denaturing secondary structures of proteins, a broad range of enveloped and nonenveloped viruses can be inactivated with heat (37, 73, 76, 77, 92). The temperature and incubation times needed to render a virus noninfective vary depending on the particular agent, although, generally, incubation at higher temperatures reduces the time required for viral inactivation. However, by denaturing protein structures, heat may also alter the conformation of virion proteins and of other microorganisms present in the sample (76, 93). Thus, lower temperatures and longer incubation times may be preferred in order to preserve microbial structures. Here, we tested incubation at 56°C for 30 min, conditions that have been proven effective against a broad battery of viruses, including MERS-CoV, SARS-CoV, and SARS-CoV-2 (37, 39, 41, 77, 94). Results showed that such incubation conditions can be detrimental to bacterial communities in some cases. While stool and skin microbiome were mostly stable after heat inactivation, nasal samples suffered significant changes in their composition. In a recent study, heat inactivation of SARS-CoV-2 at 56°C for 30 min was able to preserve reverse transcription-quantitative PCR (qRT-PCR) sensitivity to different genes of the virus (39). In a different study, however, the same protocol was shown to reduce the levels of viral RNA detection by digital PCR (38). Due to its affordability and accessibility, heat inactivation can still be a good option when working with certain microbiome samples that do not involve further immunological tests, such as antigen detection or characterization. However, heat should be generally avoided in the processing of nasal samples, a finding of high relevance in the current COVID-19 pandemic.

In our study, we observed that skin and nasal samples' bacterial communities were generally more sensitive to changes after inactivation. As discussed above, some of the approaches utilized can have detrimental effects on cell structure and nucleic acids present in the samples. Because these samples harbor low bacterial loads, there is a higher likelihood for overamplification of extraneous DNA despite rigorous quality control. On the other hand, and despite the higher loads of bacteria in stool samples, we observed that certain reagents, including ethanol, TRIZOL, and formaldehyde, depleted some important intestinal commensals, such as *Coproccoccus* or *Blautia*, while enriching others, such as *Bacteroides* or *Alistipes*. Our findings suggest that while some gut bacteria may be sensitive to specific inactivation reagents, the same reagents could improve DNA extraction of other taxa, likely due to differences in bacterial cell membrane structure. Oral samples seemed to be the most stable among those we tested. Some studies have previously reported a decrease in virucidal effectivity of certain viral inactivating agents depending on the protein content of the samples (37, 95). It is plausible that the high protein content in human saliva, including highly glycosylated mucins and proteins involved in exopolysaccharide synthesis, combined with the intricate interactions of oral bacteria with other carbohydrates and protein components of oral biofilms, could protect bacterial communities from the damaging effects of inactivation procedures (96–98).

Overall, and based on our results, we recommend the use of psoralen in combination with UV-A radiation as the inactivation agent that best preserves microbiome structure across most sample types, while we strongly discourage the use of 75% ethanol (Table 1). Although TRIZOL did not introduce major changes to oral samples, it had a larger impact on samples from other body sites. In addition, inactivation with heat

preserved stool and skin samples' community structure better than other inactivation methods but caused considerable alterations in the nasal samples, which showed better results when inactivated with formaldehyde. Thus, the use of specific inactivation methods should generally be chosen based on the type of samples under study.

There are other factors that are often considered in inactivation studies, including the concentration of the inactivating reagent and incubation conditions, as well as the specific virus to be inactivated. For example, alcohol can effectively inactivate most enveloped viruses, although some nonenveloped viruses can persist (59, 99, 100). In the study by Schneider et al., a broad range of viral agents were inactivated with psoralen in combination with UV radiation, but the amount of exposure to UV required to reach inactivation varied across viruses (88). Similarly, different temperatures and incubation times yield variable inactivation results (37–39, 77, 94). Concentration of viral particles may also be a critical factor for inactivation efficiency (101–104). In the study by Pastorino et al. (102), temperature conditions generally considered virucidal and which can inactivate a broad range of viruses were not able to inactivate SARS-CoV-2 when samples contained viral loads greater than 6-log_{10} 50% tissue culture infective dose (TCID₅₀). Viral inactivation methods may also depend on the type of assays to be performed: although next-generation sequencing does not generally require microbial cell structure integrity to be preserved, other microbiological and immunological analyses, such as serology or antigenic characterization of viruses, bacterial and viral coating with antibodies, as well as microscopy, do rely on cell integrity. In cases where molecular integrity of epitopes needs to be preserved, formaldehyde and psoralen treatments may be preferred (76, 88). It should be noted that our study only assessed the impact of inactivation in bacteria, and therefore, the potential effect on other fractions of the microbiome, such as fungal or viral communities, should be evaluated in future studies. In addition, bacterial contamination arising from laboratory reagents and kits can impact microbiome studies. When analyzing the abundance of contaminants across inactivation methods, we only identified one member of the *Bradyrhizobiaceae* family, which has been previously reported as a laboratory contaminant frequently found in DNA extraction kits and other reagents (105, 106). As we also identified this taxon in other groups, including untreated samples and samples treated with heat (which cannot be a source of microorganisms), it seems unlikely that contamination originated from the inactivating reagents. A more plausible alternative is that contaminants are introduced during regular sample processing, as previously shown (105–107). Finally, our samples were obtained from healthy subjects and do not contain infectious viruses. While the microbiome of infected patients is different from that of healthy controls (12–17), a comprehensive evaluation of all possible infection-associated microbiomes is beyond the scope of this work. Further, the use of healthy microbiomes to test the impact of storage condition or processing is well established in the literature (43, 46, 48, 108), and so, our study design follows a similar approach.

While our study did not exhaustively cover every possible inactivation agent and condition and our sample size per body site and inactivation treatment was moderate, our results clearly highlight the need to use appropriate treatments depending on the specific tissue being sampled. Larger studies using different inactivation conditions and sample types could uncover fine-grained interactions leading to the depletion or enrichment of taxa of interest. Nevertheless, we strongly encourage future studies to consider the guidelines here presented and, at a minimum, to test different inactivation protocols to ensure the robustness of their conclusions.

MATERIALS AND METHODS

Sample collection. Five healthy volunteers participated in this study. Each of them donated a stool sample in a sterile container (109), and samples were aliquoted in approximately 100-mg aliquots and frozen within 2 h of collection. A trained member of the research team collected nasal (nares), oral mucosa (inner cheek), and forearm skin specimens in a clinical setting from volunteers using sterile swabs (catalog no. 220145; BD), and samples were immediately stored at -80°C . For each subject, six swabs were collected from the oral cavity, anterior nares, and forearm skin, and six stool aliquots were made, for a total of $n = 120$ samples (Fig. 5). Sample collection for the research was approved by the

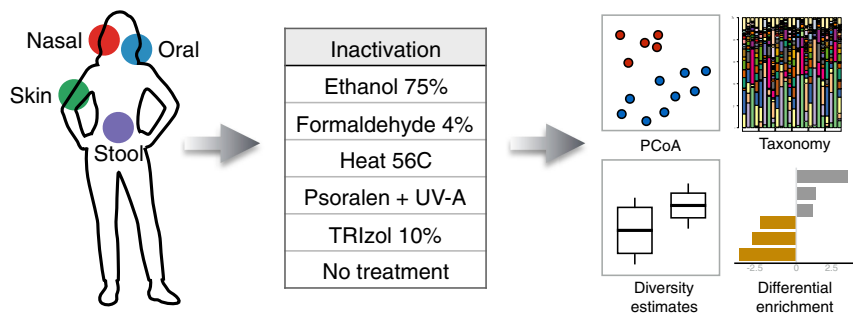


FIG 5 Study design. Forearm skin, oral, nasal, and stool specimens were obtained from five healthy subjects. Samples were aliquoted and treated with each of five inactivation methods plus an additional aliquot kept with no treatment. DNA was extracted, and 16S rRNA gene amplicons were sequenced using the Illumina MiSeq platform following standard protocols. Microbiome composition, diversity estimates, and differential enrichment analysis were performed to identify inactivation- and tissue-specific changes.

institutional review board (IRB) at The Icahn School of Medicine at Mount Sinai in New York, and all subjects signed informed consent.

Inactivation protocols. Specimens from each subject were treated with each of the following five inactivation methods: heat (39), ethanol (71), psoralen (88), TRIZol (110), and formaldehyde (79), as well as a no-treatment method consisting of immediate thawing and DNA extraction. Heat-treated samples were suspended in sterile PBS and incubated for 30 min at 56°C in a heat block (Denville Scientific). Absolute ethyl alcohol (ethanol) was diluted with PBS and added at a 75% final concentration, and samples were incubated at room temperature for 30 min. Psoralen ($\geq 99\%$; Sigma-Aldrich) was added at a final concentration of 10 $\mu\text{g}/\text{ml}$ in dimethyl sulfoxide (DMSO); samples were incubated at room temperature for 30 min and then transferred to a 24-well plate and exposed to UV radiation in a BioDoc-It imaging system (UVP) for 30 min. TRIZol reagent (Invitrogen) was added at a final concentration of 10% in sterile PBS, and samples were incubated at room temperature for 10 min. Formaldehyde was added at a final 4% concentration in PBS, and samples were incubated at room temperature for 30 min (Fig. 5).

DNA extraction and 16S rRNA gene library construction. On the same day that samples were inactivated, DNA was extracted with a DNeasy PowerLyzer PowerSoil kit (Qiagen) following the manufacturer's instructions. The concentration of extracted DNA was estimated by using a NanoDrop ND-1000 spectrophotometer (Thermo Scientific). For each sample, the V4 region of the 16S rRNA gene was amplified in triplicate, following the protocol from Caporaso et al. (111). The amplified replicates were pooled, their DNA concentration was measured using Qubit fluorometric quantitation, and sequencing was performed in an Illumina MiSeq platform (paired-end 250 bp), as previously described (111–113), at the Genomics Core at NYU (New York). This resulted in a total of 128 samples, including 8 blanks (6 DNA extraction controls, treated with each inactivation method or no treatment, and 2 PCR controls).

16S rRNA gene sequencing data analysis. The resulting raw sequencing reads were initially analyzed using QIIME2 v2020.8 (<https://qiime2.org>) (64). Reads were demultiplexed and quality filtered, and pair ends were joined with DADA2. Filtered sequences were clustered and assigned to amplicon sequence variants (ASVs) using the GreenGenes v13.8 full-length sequence database (114). Common reagent bacterial contaminants were removed following recommendations from Salter et al. (105). The list of removed contaminants can be found in Table S1 in the supplemental material. After filtering, a mean \pm SD of $45,519 \pm 33,708$ sequences per sample remained, with a mean of 84.42 ± 58 observed features per sample. One oral sample inactivated by heat yielded less than 500 reads and was eliminated from the data set. A phylogenetic tree was generated using the align-to-tree-mafft-fasttree function in QIIME2 and was used to calculate phylogeny-informed distances between samples (UniFrac distances). Alpha- and beta-diversity indices were measured on tables rarefied at 4,385 sequences per sample. All other statistical analyses were performed on R software v4.0.3 (115). Principal coordinate analysis (PCoA) and density plots based on UniFrac distances were visualized with the ggplot2 (116) package in R, and a nested permutational multivariate analysis of variance (adonis) test was applied to compare the effect size of inactivation methods and body site on beta diversity, stratifying per subject, using the adonis function from the vegan package in R with 999 permutations. To test for homogeneity of variability (dispersion) among inactivation methods and body sites, permutation multivariate analysis of dispersion was conducted with the betadisper and permutest functions, also from the vegan package. Bacterial relative abundances were summarized in barplots, using the barplot package. Linear models for alpha diversity were constructed using the glm function in the stats package in R. We used an identity link function and a Gaussian error model in accordance with the apparent distribution of the data. The input formula contains linear terms and an interaction term between body site and treatment as follows: SE (Shannon entropy) or OF (observed features) \sim subject + body + treatment + body/treatment. Coefficients with P values of <0.05 were kept in the model. Differences in composition at the phylum level were calculated as the ratio of the difference between bacterial relative abundances in each treatment compared to no treatment (fold change). Linear discriminant analysis effect size (LefSe) (55) was used to identify differentially abundant taxa between each treatment

compared to no treatment for each sample type. Kruskal-Wallis and pairwise Wilcoxon tests were used to compare differences between inactivation protocols and body sites. For all statistical analyses, a *P* value of <0.05 was considered significant. ANCOM analysis (56), as implemented in QIIME2, was applied to compare microbial taxonomic differences between blank controls treated with each inactivation method and no treatment.

Data availability. Raw sequencing data are available from the NCBI Sequence Read Archive under the BioProject accession no. [PRJNA724050](https://www.ncbi.nlm.nih.gov/bioproject/PRJNA724050).

SUPPLEMENTAL MATERIAL

Supplemental material is available online only.

FIG S1, PDF file, 0.01 MB.

FIG S2, PDF file, 0.04 MB.

FIG S3, PDF file, 0.03 MB.

FIG S4, PDF file, 0.3 MB.

FIG S5, PDF file, 0.03 MB.

TABLE S1, XLSX file, 0.1 MB.

ACKNOWLEDGMENTS

D.M. and J.C.C. were partially supported by R01MH110418. Computational analysis was partially supported by Mount Sinai's Scientific Computing through an allocation to J.C.C.

REFERENCES

- Schirmer M, Franzosa EA, Lloyd-Price J, McIver LJ, Schwager R, Poon TW, Ananthakrishnan AN, Andrews E, Barron G, Lake K, Prasad M, Sauk J, Stevens B, Wilson RG, Braun J, Denson LA, Kugathasan S, McGovern DPB, Vlamakis H, Xavier RJ, Huttenhower C. 2018. Dynamics of metatranscription in the inflammatory bowel disease gut microbiome. *Nat Microbiol* 3: 337–346. <https://doi.org/10.1038/s41564-017-0089-z>.
- Clemente JC, Manasson J, Scher JU. 2018. The role of the gut microbiome in systemic inflammatory disease. *BMJ* 360:j5145. <https://doi.org/10.1136/bmj.j5145>.
- Morgan XC, Tickle TL, Sokol H, Gevers D, Devaney KL, Ward DV, Reyes JA, Shah SA, LeLeiko N, Snapper SB, Bousvaros A, Korzenik J, Sands BE, Xavier RJ, Huttenhower C. 2012. Dysfunction of the intestinal microbiome in inflammatory bowel disease and treatment. *Genome Biol* 13: R79. <https://doi.org/10.1186/gb-2012-13-9-r79>.
- Dickson RP, Erb-Downward JR, Martinez FJ, Huffnagle GB. 2016. The microbiome and the respiratory tract. *Annu Rev Physiol* 78:481–504. <https://doi.org/10.1146/annurev-physiol-021115-105238>.
- Budden KF, Gellatly SL, Wood DLA, Cooper MA, Morrison M, Hugenholtz P, Hansbro PM. 2017. Emerging pathogenic links between microbiota and the gut-lung axis. *Nat Rev Microbiol* 15:55–63. <https://doi.org/10.1038/nrmicro.2016.142>.
- Plunkett CH, Nagler CR. 2017. The influence of the microbiome on allergic sensitization to food. *J Immunol* 198:581–589. <https://doi.org/10.4049/jimmunol.1601266>.
- Fujimura KE, Lynch SV. 2015. Microbiota in allergy and asthma and the emerging relationship with the gut microbiome. *Cell Host Microbe* 17: 592–602. <https://doi.org/10.1016/j.chom.2015.04.007>.
- Frati F, Salvaroli C, Incorvaia C, Bellucci A, Di Cara G, Maruccci F, Esposito S. 2018. The role of the microbiome in asthma: the gut-lung axis. *Int J Mol Sci* 20. <https://doi.org/10.3390/ijms20010123>.
- Morais LH, Schreiber HL, Mazmanian SK. 2021. The gut microbiota–brain axis in behaviour and brain disorders. *Nat Rev Microbiol* 19:241–255. <https://doi.org/10.1038/s41579-020-00460-0>.
- Cryan JF, O'Mahony SM. 2011. The microbiome-gut-brain axis: from bowel to behavior. *Neurogastroenterol Motil* 23:187–192. <https://doi.org/10.1111/j.1365-2982.2010.01664.x>.
- Foster JA, McVey Neufeld K-A. 2013. Gut–brain axis: how the microbiome influences anxiety and depression. *Trends Neurosci* 36:305–312. <https://doi.org/10.1016/j.tins.2013.01.005>.
- Kaul D, Rathnasinghe R, Ferres M, Tan GS, Barrera A, Pickett BE, Methe BA, Das SR, Budnik I, Halpin RA, Wentworth D, Schmolke M, Mena I, Albrecht RA, Singh I, Nelson KE, García-Sastre A, Dupont CL, Medina RA. 2020. Microbiome disturbance and resilience dynamics of the upper respiratory tract during influenza A virus infection. *Nat Commun* 11: 2537. <https://doi.org/10.1038/s41467-020-16429-9>.
- Wang J, Li F, Wei H, Lian ZX, Sun R, Tian Z. 2014. Respiratory influenza virus infection induces intestinal immune injury via microbiota-mediated Th17 cell-dependent inflammation. *J Exp Med* 211:2397–2410. <https://doi.org/10.1084/jem.20140625>.
- Yildiz S, Mazel-Sanchez B, Kandasamy M, Manicassamy B, Schmolke M. 2018. Influenza A virus infection impacts systemic microbiota dynamics and causes quantitative enteric dysbiosis. *Microbiome* 6:9. <https://doi.org/10.1186/s40168-017-0386-z>.
- McHardy IH, Li X, Tong M, Ruegger P, Jacobs J, Borneman J, Anton P, Braun J. 2013. HIV infection is associated with compositional and functional shifts in the rectal mucosal microbiota. *Microbiome* 1:26. <https://doi.org/10.1186/2049-2618-1-26>.
- Gu S, Chen Y, Wu Z, Chen Y, Gao H, Lv L, Guo F, Zhang X, Luo R, Huang C, Lu H, Zheng B, Zhang J, Yan R, Zhang H, Jiang H, Xu Q, Guo J, Gong Y, Tang L, Li L. 2020. Alterations of the gut microbiota in patients with COVID-19 or H1N1 influenza. *Clin Infect Dis* 71:2669–2678. <https://doi.org/10.1093/cid/ciaa709>.
- Zuo T, Zhang F, Lui GCY, Yeoh YK, Li AYL, Zhan H, Wan Y, Chung ACK, Cheung CP, Chen N, Lai CKC, Chen Z, Tso EYK, Fung KSC, Chan V, Ling L, Joynt G, Hui DSC, Chan FKL, Chan PKS, Ng SC. 2020. Alterations in gut microbiota of patients with COVID-19 during time of hospitalization. *Gastroenterology* 159:944–955.e8. <https://doi.org/10.1053/j.gastro.2020.05.048>.
- Yaron JR, Ambadapadi S, Zhang L, Chavan RN, Tibbetts SA, Keinan S, Varsani A, Maldonado J, Kraberger S, Tafoya AM, Bullard WL, Kilbourne J, Stern-Harbutte A, Krajmalnik-Brown R, Munk BH, Koppang EO, Lim ES, Lucas AR. 2020. Immune protection is dependent on the gut microbiome in a lethal mouse gammaherpesviral infection. *Sci Rep* 10:2371. <https://doi.org/10.1038/s41598-020-59269-9>.
- Thackray LB, Handley SA, Gorman MJ, Poddar S, Bagadia P, Briseño CG, Theisen DJ, Tan Q, Hykes BL, Jr., Lin H, Lucas TM, Desai C, Gordon JI, Murphy KM, Virgin HW, Diamond MS. 2018. Oral antibiotic treatment of mice exacerbates the disease severity of multiple flavivirus infections. *Cell Rep* 22:3440–3453.e6. <https://doi.org/10.1016/j.celrep.2018.03.001>.
- Rigo-Adrover MDM, van Limpt K, Knipping K, Garssen J, Knol J, Costabile A, Franch À, Castell M, Pérez-Cano FJ. 2018. Preventive effect of a symbiotic combination of galacto- and fructooligosaccharides mixture with *Bifidobacterium breve* M-16V in a model of multiple rotavirus infections. *Front Immunol* 9:1318. <https://doi.org/10.3389/fimmu.2018.01318>.
- Park MK, Ngo V, Kwon YM, Lee YT, Yoo S, Cho YH, Hong SM, Hwang HS, Ko EJ, Jung YJ, Moon DW, Jeong EJ, Kim MC, Lee YN, Jang JH, Oh JS, Kim CH, Kang SM. 2013. *Lactobacillus plantarum* DK119 as a probiotic confers

- protection against influenza virus by modulating innate immunity. *PLoS One* 8:e75368. <https://doi.org/10.1371/journal.pone.0075368>.
22. Oh JE, Kim BC, Chang DH, Kwon M, Lee SY, Kang D, Kim JY, Hwang I, Yu JW, Nakae S, Lee HK. 2016. Dysbiosis-induced IL-33 contributes to impaired antiviral immunity in the genital mucosa. *Proc Natl Acad Sci U S A* 113:E762–E771. <https://doi.org/10.1073/pnas.1518589113>.
 23. Erickson AK, Jesudhasan PR, Mayer MJ, Narbad A, Winter SE, Pfeiffer JK. 2018. Bacteria facilitate enteric virus co-infection of mammalian cells and promote genetic recombination. *Cell Host Microbe* 23:77–88.e5. <https://doi.org/10.1016/j.chom.2017.11.007>.
 24. Li N, Ma W-T, Pang M, Fan Q-L, Hua J-L. 2019. The commensal microbiota and viral infection: a comprehensive review. *Front Immunol* 10:1551–1551. <https://doi.org/10.3389/fimmu.2019.01551>.
 25. Benedikz EK, Bailey D, Cook CNL, Gonçalves-Carneiro D, Buckner MMC, Blair JMA, Wells TJ, Fletcher NF, Goodall M, Flores-Langarica A, Kingsley RA, Madsen J, Teeling J, Johnston SL, MacLennan CA, Balfe P, Henderson IR, Piddock LJV, Cunningham AF, McKeating JA. 2019. Bacterial flagellin promotes viral entry via an NF- κ B and Toll like receptor 5 dependent pathway. *Sci Rep* 9:7903. <https://doi.org/10.1038/s41598-019-44263-7>.
 26. Jones MK, Watanabe M, Zhu S, Graves CL, Keyes LR, Grau KR, Gonzalez-Hernandez MB, Iovine NM, Wobus CE, Vinjé J, Tibbetts SA, Wallet SM, Karst SM. 2014. Enteric bacteria promote human and mouse norovirus infection of B cells. *Science* 346:755–759. <https://doi.org/10.1126/science.1257147>.
 27. Baldridge MT, Nice TJ, McCune BT, Yokoyama CC, Kambal A, Wheldon M, Diamond MS, Ivanova Y, Artyomov M, Virgin HW. 2015. Commensal microbes and interferon- λ determine persistence of enteric murine norovirus infection. *Science* 347:266–269. <https://doi.org/10.1126/science.1258025>.
 28. Itoh Y, Shinya K, Kiso M, Watanabe T, Sakoda Y, Hatta M, Muramoto Y, Tamura D, Sakai-Tagawa Y, Noda T, Sakabe S, Imai M, Hatta Y, Watanabe S, Li C, Yamada S, Fujii K, Murakami S, Imai H, Kakugawa S, Ito M, Takano R, Iwatsuki-Horimoto K, Shimajima M, Horimoto T, Goto H, Takahashi K, Makino A, Ishigaki H, Nakayama M, Okamatsu M, Takahashi K, Warshauer D, Shult PA, Saito R, Suzuki H, Furuta Y, Yamashita M, Mitamura K, Nakano K, Nakamura M, Brockman-Schneider R, Mitamura H, Yamazaki M, Sugaya N, Suresh M, Ozawa M, Neumann G, Gern J, Kida H, et al. 2009. In vitro and in vivo characterization of new swine-origin H1N1 influenza viruses. *Nature* 460:1021–1025. <https://doi.org/10.1038/nature08260>.
 29. Sun H, Xiao Y, Liu J, Wang D, Li F, Wang C, Li C, Zhu J, Song J, Sun H, Jiang Z, Liu L, Zhang X, Wei K, Hou D, Pu J, Sun Y, Tong Q, Bi Y, Chang K-C, Liu S, Gao GF, Liu J. 2020. Prevalent Eurasian avian-like H1N1 swine influenza virus with 2009 pandemic viral genes facilitating human infection. *Proc Natl Acad Sci U S A* 117:17204–17210. <https://doi.org/10.1073/pnas.1921186117>.
 30. Kuiken T, Fouchier RA, Schutten M, Rimmelzwaan GF, van Amerongen G, van Riel D, Laman JD, de Jong T, van Doornum G, Lim W, Ling AE, Chan PK, Tam JS, Zambon MC, Gopal R, Drost C, van der Werf S, Escriou N, Manuguerra JC, Stöhr K, Peiris JS, Osterhaus AD. 2003. Newly discovered coronavirus as the primary cause of severe acute respiratory syndrome. *Lancet* 362:263–270. [https://doi.org/10.1016/S0140-6736\(03\)13967-0](https://doi.org/10.1016/S0140-6736(03)13967-0).
 31. Ksiazek TG, Erdman D, Goldsmith CS, Zaki SR, Peret T, Emery S, Tong S, Urbani C, Comer JA, Lim W, Rollin PE, Dowell SF, Ling AE, Humphrey CD, Shieh WJ, Guarner J, Paddock CD, Rota P, Fields B, DeRisi J, Yang JY, Cox N, Hughes JM, LeDuc JW, Bellini WJ, Anderson LJ, SARS Working Group. 2003. A novel coronavirus associated with severe acute respiratory syndrome. *N Engl J Med* 348:1953–1966. <https://doi.org/10.1056/NEJMoa030781>.
 32. Azhar EI, El-Kafrawy SA, Farraj SA, Hassan AM, Al-Saeed MS, Hashem AM, Madani TA. 2014. Evidence for camel-to-human transmission of MERS coronavirus. *N Engl J Med* 370:2499–2505. <https://doi.org/10.1056/NEJMoa1401505>.
 33. Memish ZA, Perlman S, Van Kerkhove MD, Zumla A. 2020. Middle East respiratory syndrome. *Lancet* 395:1063–1077. [https://doi.org/10.1016/S0140-6736\(19\)33221-0](https://doi.org/10.1016/S0140-6736(19)33221-0).
 34. Chen N, Zhou M, Dong X, Qu J, Gong F, Han Y, Qiu Y, Wang J, Liu Y, Wei Y, Xia J, Yu T, Zhang X, Zhang L. 2020. Epidemiological and clinical characteristics of 99 cases of 2019 novel coronavirus pneumonia in Wuhan, China: a descriptive study. *Lancet* 395:507–513. [https://doi.org/10.1016/S0140-6736\(20\)30211-7](https://doi.org/10.1016/S0140-6736(20)30211-7).
 35. Lai C-C, Shih T-P, Ko W-C, Tang H-J, Hsueh P-R. 2020. Severe acute respiratory syndrome coronavirus 2 (SARS-CoV-2) and coronavirus disease-2019 (COVID-19): the epidemic and the challenges. *Int J Antimicrob Agents* 55:105924. <https://doi.org/10.1016/j.ijantimicag.2020.105924>.
 36. Chosewood L, Wilson D. 2009. Biosafety in microbiological and biomedical laboratories, 5th ed. Centers for Disease Control and Prevention, Atlanta, GA.
 37. Darnell ME, Taylor DR. 2006. Evaluation of inactivation methods for severe acute respiratory syndrome coronavirus in noncellular blood products. *Transfusion* 46:1770–1777. <https://doi.org/10.1111/j.1537-2995.2006.00976.x>.
 38. Chen H, Wu R, Xing Y, Du Q, Xue Z, Xi Y, Yang Y, Deng Y, Han Y, Li K, Luan Y, Zhang Y, Wei X, Yu T, Li H, Zhu L, Su S, Lian H, Lu L, Tan C, Zheng H, Chen B, Yu P, Guo Y, Ma C. 2020. Influence of different inactivation methods on severe acute respiratory syndrome coronavirus 2 RNA copy number. *J Clin Microbiol* 58:e00958-20. <https://doi.org/10.1128/JCM.00958-20>.
 39. Kim YI, Casel MAB, Kim SM, Kim SG, Park SJ, Kim EH, Jeong HW, Poo H, Choi YK. 2020. Development of severe acute respiratory syndrome coronavirus 2 (SARS-CoV-2) thermal inactivation method with preservation of diagnostic sensitivity. *J Microbiol* 58:886–891. <https://doi.org/10.1007/s12275-020-0335-6>.
 40. Patterson EI, Prince T, Anderson ER, Casas-Sanchez A, Smith SL, Cansado-Utrilla C, Solomon T, Griffiths MJ, Acosta-Serrano Á, Turtle L, Hughes GL. 2020. Methods of inactivation of SARS-CoV-2 for downstream biological assays. *J Infect Dis* 222:1462–1467. <https://doi.org/10.1093/infdis/jiaa507>.
 41. Batéjat C, Grassin Q, Manuguerra J-C, Leclercq I. 2020. Heat inactivation of the severe acute respiratory syndrome coronavirus 2. *J Biosaf Biosecur* 3:1–3. <https://doi.org/10.1016/j.jjobb.2020.12.001>.
 42. Gorzelak MA, Gill SK, Tasnim N, Ahmadi-Vand Z, Jay M, Gibson DL. 2015. Methods for improving human gut microbiome data by reducing variability through sample processing and storage of stool. *PLoS One* 10:e0134802. <https://doi.org/10.1371/journal.pone.0134802>.
 43. Song SJ, Amir A, Metcalf JL, Amato KR, Xu ZZ, Humphrey G, Knight R. 2016. Preservation methods differ in fecal microbiome stability, affecting suitability for field studies. *mSystems* 1:e00021-16. <https://doi.org/10.1128/mSystems.00021-16>.
 44. Tatangelo V, Franzetti A, Gandolfi I, Bestetti G, Ambrosini R. 2014. Effect of preservation method on the assessment of bacterial community structure in soil and water samples. *FEMS Microbiol Lett* 356:32–38. <https://doi.org/10.1111/1574-6968.12475>.
 45. Menke S, Gillingham MA, Wilhelm K, Sommer S. 2017. Home-made cost effective preservation buffer is a better alternative to commercial preservation methods for microbiome research. *Front Microbiol* 8:102. <https://doi.org/10.3389/fmicb.2017.00102>.
 46. Jenkins SV, Vang KB, Gies A, Griffin RJ, Jun S-R, Nookaew I, Dings RPM. 2018. Sample storage conditions induce post-collection biases in microbiome profiles. *BMC Microbiol* 18:227. <https://doi.org/10.1186/s12866-018-1359-5>.
 47. Shaw AG, Sim K, Powell E, Cornwell E, Cramer T, McClure ZE, Li MS, Kroll JS. 2016. Latitude in sample handling and storage for infant faecal microbiota studies: the elephant in the room? *Microbiome* 4:40. <https://doi.org/10.1186/s40168-016-0186-x>.
 48. Pribyl AL, Parks DH, Angel NZ, Boyd JA, Hasson AG, Fang L, MacDonald SL, Wills BA, Wood DLA, Krause L, Tyson GW, Hugenholtz P. 2021. Critical evaluation of faecal microbiome preservation using metagenomic analysis. *Isme Commun* 1:14. <https://doi.org/10.1038/s43705-021-00014-2>.
 49. Sagripanti J-L, Hülseweh B, Grote G, Voss L, Böhring K, Marschall H-J. 2011. Microbial inactivation for safe and rapid diagnostics of infectious samples. *Appl Environ Microbiol* 77:7289–7295. <https://doi.org/10.1128/AEM.05553-11>.
 50. Lee KH, Gordon A, Shedden K, Kuan G, Ng S, Balmaseda A, Foxman B. 2019. The respiratory microbiome and susceptibility to influenza virus infection. *PLoS One* 14:e0207898. <https://doi.org/10.1371/journal.pone.0207898>.
 51. Britton GJ, Chen-Liaw A, Cossarini F, Livanos AE, Spindler MP, Plitt T, Eggers J, Mogno I, Gonzalez-Reiche AS, Siu S, Tankelevich M, Tal Grinspan L, Dixon RE, Jha D, van de Guchte A, Khan Z, Martinez-Delgado G, Amanat F, Hoagland DA, tenOever BR, Dubinsky MC, Merad M, van Bakel H, Krammer F, Bongers G, Mehndru S, Faith JJ. 2021. Limited intestinal inflammation despite diarrhea, fecal viral RNA and SARS-CoV-2-specific IgA in patients with acute COVID-19. *Sci Rep* 11:13308. <https://doi.org/10.1038/s41598-021-92740-9>.
 52. Yeoh YK, Zuo T, Lui GC-Y, Zhang F, Liu Q, Li AY, Chung AC, Cheung CP, Tso EY, Fung KS, Chan V, Ling L, Joynt G, Hui DS-C, Chow KM, Ng SSS, Li TC-M, Ng RW, Yip TC, Wong GL-H, Chan FK, Wong CK, Chan PK, Ng SC. 2021. Gut microbiota composition reflects disease severity and dysfunctional immune responses in patients with COVID-19. *Gut* 70:698–706. <https://doi.org/10.1136/gutjnl-2020-323020>.
 53. Ward DV, Bhattarai S, Rojas-Correa M, Purkayastha A, Holler D, Da Qu M, Mitchell WG, Yang J, Fountain S, Zeamer A, Forconi C, Fujimori G, Odwar B, Cawley C, McCormick BA, Moormann A, Wessolossky M, Bucci V, Maldonado-Contreras A. 2021. The intestinal and oral microbiomes are

- robust predictors of covid-19 severity the main predictor of COVID-19-related fatality. medRxiv <https://doi.org/10.1101/2021.01.05.20249061>: 2021.01.05.20249061.
54. Costello EK, Lauber CL, Hamady M, Fierer N, Gordon JL, Knight R. 2009. Bacterial community variation in human body habitats across space and time. *Science* 326:1694–1697. <https://doi.org/10.1126/science.1177486>.
 55. Segata N, Izard J, Waldron L, Gevers D, Miropolsky L, Garrett WS, Huttenhower C. 2011. Metagenomic biomarker discovery and explanation. *Genome Biol* 12:R60. <https://doi.org/10.1186/gb-2011-12-6-r60>.
 56. Mandal S, Van Treuren W, White RA, Eggesbø M, Knight R, Peddada SD. 2015. Analysis of composition of microbiomes: a novel method for studying microbial composition. *Microb Ecol Health Dis* 26:27663. <https://doi.org/10.3402/mehd.v26.27663>.
 57. Fierer N, Lauber CL, Zhou N, McDonald D, Costello EK, Knight R. 2010. Forensic identification using skin bacterial communities. *Proc Natl Acad Sci U S A* 107:6477–6481. <https://doi.org/10.1073/pnas.1000162107>.
 58. The Human Microbiome Project Consortium. 2012. Structure, function and diversity of the healthy human microbiome. *Nature* 486:207–214. <https://doi.org/10.1038/nature11234>.
 59. Rutala WA, Weber DJ. 2008. Guideline for disinfection and sterilization in healthcare facilities, 2008. Centers for Disease Control and Prevention, Atlanta, GA.
 60. Smither SJ, Weller SA, Phelps A, Eastaugh L, Ngugi S, O'Brien LM, Steward J, Lonsdale SG, Lever MS. 2015. Buffer AVL alone does not inactivate Ebola virus in a representative clinical sample type. *J Clin Microbiol* 53:3148–3154. <https://doi.org/10.1128/JCM.01449-15>.
 61. Chedore P, Th'ng C, Nolan DH, Churchwell GM, Sieffert DE, Hale YM, Jamieson F. 2002. Method for inactivating and fixing unstained smear preparations of *Mycobacterium tuberculosis* for improved laboratory safety. *J Clin Microbiol* 40:4077–4080. <https://doi.org/10.1128/JCM.40.11.4077-4080.2002>.
 62. Krafft AE, Russell KL, Hawksworth AW, McCall S, Irvine M, Daum LT, Connolly JL, Reid AH, Gaydos JC, Taubenberger JK. 2005. Evaluation of PCR testing of ethanol-fixed nasal swab specimens as an augmented surveillance strategy for influenza virus and adenovirus identification. *J Clin Microbiol* 43:1768–1775. <https://doi.org/10.1128/JCM.43.4.1768-1775.2005>.
 63. Luinstra K, Petrich A, Castriciano S, Ackerman M, Chong S, Carruthers S, Ammons B, Mahony JB, Smieja M. 2011. Evaluation and clinical validation of an alcohol-based transport medium for preservation and inactivation of respiratory viruses. *J Clin Microbiol* 49:2138–2142. <https://doi.org/10.1128/JCM.00327-11>.
 64. Bolyen E, Rideout JR, Dillon MR, Bokulich NA, Abnet CC, Al-Ghalith GA, Alexander H, Alm EJ, Arumugam M, Anisic F, Bai Y, Bisanz JE, Bittinger K, Brejnrod A, Brislawn CJ, Brown CT, Callahan BJ, Caraballo-Rodríguez AM, Chase J, Cope EK, Da Silva R, Diener C, Dorrestein PC, Douglas GM, Durall DM, Duvallet C, Edwardson CF, Ernst M, Estaki M, Fouquier J, Gauglitz JM, Gibbons SM, Gibson DL, Gonzalez A, Gorlick K, Guo J, Hillmann B, Holmes S, Holste H, Huttenhower C, Huttley GA, Janssen S, Jarmusch AK, Jiang L, Kaehler BD, Kang KB, Keefe CR, Keim P, Kelley ST, Knights D, et al. 2019. Reproducible, interactive, scalable and extensible microbiome data science using QIIME 2. *Nat Biotechnol* 37:852–857. <https://doi.org/10.1038/s41587-019-0209-9>.
 65. Hale VL, Tan CL, Knight R, Amato KR. 2015. Effect of preservation method on spider monkey (*Ateles geoffroyi*) fecal microbiota over 8 weeks. *J Microbiol Methods* 113:16–26. <https://doi.org/10.1016/j.mimet.2015.03.021>.
 66. Vlčková K, Mrázek J, Kopečný J, Petrželková KJ. 2012. Evaluation of different storage methods to characterize the fecal bacterial communities of captive western lowland gorillas (*Gorilla gorilla gorilla*). *J Microbiol Methods* 91:45–51. <https://doi.org/10.1016/j.mimet.2012.07.015>.
 67. Meyers C, Kass R, Goldenberg D, Milici J, Alam S, Robison R. 2021. Ethanol and isopropanol inactivation of human coronavirus on hard surfaces. *J Hosp Infect* 107:45–49. <https://doi.org/10.1016/j.jhin.2020.09.026>.
 68. Macinga DR, Sattar SA, Jaykus L-A, Arbogast JW. 2008. Improved inactivation of nonenveloped enteric viruses and their surrogates by a novel alcohol-based hand sanitizer. *Appl Environ Microbiol* 74:5047–5052. <https://doi.org/10.1128/AEM.00487-08>.
 69. National Health Commission & State Administration of Traditional Chinese Medicine. 2020. Diagnosis and treatment protocol for novel coronavirus pneumonia (trial version 7). *Chin Med J* 133:1087–1095. <https://doi.org/10.1097/CM9.0000000000000819>.
 70. Kariwa H, Fujii N, Takashima I. 2006. Inactivation of SARS coronavirus by means of povidone-iodine, physical conditions and chemical reagents. *Dermatology* 212(Suppl 1):119–123. <https://doi.org/10.1159/000089211>.
 71. Kratzel A, Todt D, V'Kovski P, Steiner S, Gultom M, Thao TTN, Ebert N, Holwerda M, Steinmann J, Niemeyer D, Dijkman R, Kampf G, Drosten C, Steinmann E, Thiel V, Pfaender S. 2020. Inactivation of severe acute respiratory syndrome coronavirus 2 by WHO-recommended hand rub formulations and alcohols. *Emerg Infect Dis* 26:1592–1595. <https://doi.org/10.3201/eid2607.200915>.
 72. Kumar M, Mazur S, Ork BL, Postnikova E, Hensley LE, Jahrling PB, Johnson R, Holbrook MR. 2015. Inactivation and safety testing of Middle East respiratory syndrome coronavirus. *J Virol Methods* 223:13–18. <https://doi.org/10.1016/j.jviromet.2015.07.002>.
 73. Jureka AS, Silvas JA, Basler CF. 2020. Propagation, inactivation, and safety testing of SARS-CoV-2. *Viruses* 12:622. <https://doi.org/10.3390/v12060622>.
 74. Blow JA, Dohm DJ, Negley DL, Mores CN. 2004. Virus inactivation by nucleic acid extraction reagents. *J Virol Methods* 119:195–198. <https://doi.org/10.1016/j.jviromet.2004.03.015>.
 75. Xu Q, Gill S, Xu L, Gonzalez E, Pichichero ME. 2019. Comparative analysis of microbiome in nasopharynx and middle ear in young children with acute otitis media. *Front Genet* 10:1176. <https://doi.org/10.3389/fgene.2019.01176>.
 76. Jonges M, Liu WM, van der Vries E, Jacobi R, Pronk I, Boog C, Koopmans M, Meijer A, Soethout E. 2010. Influenza virus inactivation for studies of antigenicity and phenotypic neuraminidase inhibitor resistance profiling. *J Clin Microbiol* 48:928–940. <https://doi.org/10.1128/JCM.02045-09>.
 77. Darnell ME, Subbarao K, Feinstone SM, Taylor DR. 2004. Inactivation of the coronavirus that induces severe acute respiratory syndrome, SARS-CoV. *J Virol Methods* 121:85–91. <https://doi.org/10.1016/j.jviromet.2004.06.006>.
 78. Jiang W, Schwendeman SP. 2000. Formaldehyde-mediated aggregation of protein antigens: comparison of untreated and formalinized model antigens. *Biotechnol Bioeng* 70:507–517. [https://doi.org/10.1002/1097-0290\(20001205\)70:5<507::AID-BIT5>3.0.CO;2-C](https://doi.org/10.1002/1097-0290(20001205)70:5<507::AID-BIT5>3.0.CO;2-C).
 79. Möller L, Schünadel L, Nitsche A, Schwebke I, Hanisch M, Laue M. 2015. Evaluation of virus inactivation by formaldehyde to enhance biosafety of diagnostic electron microscopy. *Viruses* 7:666–679. <https://doi.org/10.3390/v7020666>.
 80. Wilton T, Dunn G, Eastwood D, Minor PD, Martin J. 2014. Effect of formaldehyde inactivation on poliovirus. *J Virol* 88:11955–11964. <https://doi.org/10.1128/JVI.01809-14>.
 81. Delrue I, Delputte PL, Nauwynck HJ. 2009. Assessing the functionality of viral entry-associated domains of porcine reproductive and respiratory syndrome virus during inactivation procedures, a potential tool to optimize inactivated vaccines. *Vet Res* 40:62. <https://doi.org/10.1051/vetres/2009047>.
 82. Brown F. 1993. Review of accidents caused by incomplete inactivation of viruses. *Dev Biol Stand* 81:103–107.
 83. Sagripanti JL, Eklund CA, Trost PA, Jinneman KC, Abeyta C, Jr., Kaysner CA, Hill WE. 1997. Comparative sensitivity of 13 species of pathogenic bacteria to seven chemical germicides. *Am J Infect Control* 25:335–339. [https://doi.org/10.1016/S0196-6553\(97\)90026-2](https://doi.org/10.1016/S0196-6553(97)90026-2).
 84. Loibner M, Buzina W, Viertler C, Groelz D, Hausleitner A, Sialylyte G, Kufferath I, Kölli B, Zatloukal K. 2016. Pathogen inactivating properties and increased sensitivity in molecular diagnostics by PAXgene, a novel non-crosslinking tissue fixative. *PLoS One* 11:e0151383. <https://doi.org/10.1371/journal.pone.0151383>.
 85. Rocha R, Almeida C, Azevedo NF. 2018. Influence of the fixation/permeabilization step on peptide nucleic acid fluorescence in situ hybridization (PNA-FISH) for the detection of bacteria. *PLoS One* 13:e0196522. <https://doi.org/10.1371/journal.pone.0196522>.
 86. Raviprakash K, Sun P, Raviv Y, Luke T, Martin N, Kochel T. 2013. Dengue virus photo-inactivated in presence of 1,5-iodonaphthylazide (INA) or AMT, a psoralen compound (4'-aminomethyl-trioxsalen) is highly immunogenic in mice. *Hum Vaccin Immunother* 9:2336–2341. <https://doi.org/10.4161/hv.25602>.
 87. Groene WS, Shaw RD. 1992. Psoralen preparation of antigenically intact noninfectious rotavirus particles. *J Virol Methods* 38:93–102. [https://doi.org/10.1016/0166-0934\(92\)90172-a](https://doi.org/10.1016/0166-0934(92)90172-a).
 88. Schneider K, Wronka-Edwards L, Leggett-Embrey M, Walker E, Sun P, Ondov B, Wyman TH, Rosovitz MJ, Bohn SS, Burans J, Kochel T. 2015. Psoralen inactivation of viruses: a process for the safe manipulation of viral antigen and nucleic acid. *Viruses* 7:5875–5888. <https://doi.org/10.3390/v7112912>.

89. Maves RC, Oré RM, Porter KR, Kochel TJ. 2011. Immunogenicity and protective efficacy of a psoralen-inactivated dengue-1 virus vaccine candidate in *Aotus nancymaae* monkeys. *Vaccine* 29:2691–2696. <https://doi.org/10.1016/j.vaccine.2011.01.077>.
90. Almutawa F, Alnomair N, Wang Y, Hamzavi I, Lim HW. 2013. Systematic review of UV-based therapy for psoriasis. *Am J Clin Dermatol* 14:87–109. <https://doi.org/10.1007/s40257-013-0015-y>.
91. Bulat V, Situm M, Dediol I, Ljubicić I, Bradić L. 2011. The mechanisms of action of phototherapy in the treatment of the most common dermatoses. *Coll Antropol* 35(Suppl 2):147–151.
92. Edwards S. 2000. Survival and inactivation of classical swine fever virus. *Vet Microbiol* 73:175–181. [https://doi.org/10.1016/s0378-1135\(00\)00143-7](https://doi.org/10.1016/s0378-1135(00)00143-7).
93. Hu X, An T, Situ B, Hu Y, Ou Z, Li Q, He X, Zhang Y, Tian P, Sun D, Rui Y, Wang Q, Ding D, Zheng L. 2020. Heat inactivation of serum interferes with the immunoanalysis of antibodies to SARS-CoV-2. *J Clin Lab Anal* 34:e23411. <https://doi.org/10.1002/jcla.23411>.
94. Leclercq I, Batéjat C, Burguière AM, Manuguerra JC. 2014. Heat inactivation of the Middle East respiratory syndrome coronavirus. *Influenza Other Respir Viruses* 8:585–586. <https://doi.org/10.1111/irv.12261>.
95. Rabenau HF, Cinatl J, Morgenstern B, Bauer G, Preiser W, Doerr HW. 2005. Stability and inactivation of SARS coronavirus. *Med Microbiol Immunol* 194:1–6. <https://doi.org/10.1007/s00430-004-0219-0>.
96. Belda-Ferre P, Williamson J, Simón-Soro Á, Artacho A, Jensen ON, Mira A. 2015. The human oral metaproteome reveals potential biomarkers for caries disease. *Proteomics* 15:3497–3507. <https://doi.org/10.1002/pmic.201400600>.
97. Grassl N, Kulak NA, Pichler G, Geyer PE, Jung J, Schubert S, Sinitcyn P, Cox J, Mann M. 2016. Ultra-deep and quantitative saliva proteome reveals dynamics of the oral microbiome. *Genome Med* 8:44. <https://doi.org/10.1186/s13073-016-0293-0>.
98. Kolenbrander PE, Palmer RJ, Jr., Periasamy S, Jakubovics NS. 2010. Oral multispecies biofilm development and the key role of cell-cell distance. *Nat Rev Microbiol* 8:471–480. <https://doi.org/10.1038/nrmicro2381>.
99. Tyler R, Ayliffe GA, Bradley C. 1990. Virucidal activity of disinfectants: studies with the poliovirus. *J Hosp Infect* 15:339–345. [https://doi.org/10.1016/0195-6701\(90\)90090-b](https://doi.org/10.1016/0195-6701(90)90090-b).
100. Mbithi JN, Springthorpe VS, Sattar SA. 1990. Chemical disinfection of hepatitis A virus on environmental surfaces. *Appl Environ Microbiol* 56:3601–3604. <https://doi.org/10.1128/aem.56.11.3601-3604.1990>.
101. Saknimit M, Inatsuki I, Sugiyama Y, Yagami K. 1988. Virucidal efficacy of physico-chemical treatments against coronaviruses and parvoviruses of laboratory animals. *Jikken Dobutsu* 37:341–345. https://doi.org/10.1538/expanim1978.37.3_341.
102. Pastorino B, Touret F, Gilles M, de Lamballerie X, Charrel RN. 2020. Heat inactivation of different types of SARS-CoV-2 samples: what protocols for biosafety, molecular detection and serological diagnostics? *Viruses* 12:735. <https://doi.org/10.3390/v12070735>.
103. Chida AS, Goldstein JM, Lee J, Tang X, Bedi K, Herzegh O, Moon JL, Petway D, Bagarozzi DA, Hughes LJ. 2021. Comparison of Zika virus inactivation methods for reagent production and disinfection methods. *J Virol Methods* 287:114004. <https://doi.org/10.1016/j.jviromet.2020.114004>.
104. Welch SR, Davies KA, Buczkowski H, Hettiarachchi N, Green N, Arnold U, Jones M, Hannah MJ, Evans R, Burton C, Burton JE, Guiver M, Cane PA, Woodford N, Bruce CB, Roberts ADG, Killip MJ. 2020. Analysis of inactivation of SARS-CoV-2 by specimen transport media, nucleic acid extraction reagents, detergents, and fixatives. *J Clin Microbiol* 58:e01713–20. <https://doi.org/10.1128/JCM.01713-20>.
105. Salter SJ, Cox MJ, Turek EM, Calus ST, Cookson WO, Moffatt MF, Turner P, Parkhill J, Loman NJ, Walker AW. 2014. Reagent and laboratory contamination can critically impact sequence-based microbiome analyses. *BMC Biol* 12:87. <https://doi.org/10.1186/s12915-014-0087-z>.
106. Laurence M, Hatzis C, Brash DE. 2014. Common contaminants in next-generation sequencing that hinder discovery of low-abundance microbes. *PLoS One* 9:e97876. <https://doi.org/10.1371/journal.pone.0097876>.
107. Glassing A, Dowd SE, Galandiuk S, Davis B, Chiodini RJ. 2016. Inherent bacterial DNA contamination of extraction and sequencing reagents may affect interpretation of microbiota in low bacterial biomass samples. *Gut Pathog* 8:24–24. <https://doi.org/10.1186/s13099-016-0103-7>.
108. Sinha R, Abu-Ali G, Vogtmann E, Fodor AA, Ren B, Amir A, Schwager E, Crabtree J, Ma S, Abnet CC, Knight R, White O, Huttenhower C, Microbiome Quality Control Project Consortium. 2017. Assessment of variation in microbial community amplicon sequencing by the Microbiome Quality Control (MBQC) project consortium. *Nat Biotechnol* 35:1077–1086. <https://doi.org/10.1038/nbt.3981>.
109. Hirten RP, Grinspan A, Fu SC, Luo Y, Suarez-Farinas M, Rowland J, Contijoch EJ, Mogno I, Yang N, Luong T, Labrias PR, Peter I, Cho JH, Sands BE, Colombel JF, Faith JJ, Clemente JC. 2019. Microbial engraftment and efficacy of fecal microbiota transplant for *Clostridium difficile* in patients with and without inflammatory bowel disease. *Inflamm Bowel Dis* 25:969–979. <https://doi.org/10.1093/ibd/izy398>.
110. Kochel TJ, Kocher GA, Ksiazek TG, Burans JP. 2017. Evaluation of TRIzol LS inactivation of viruses. *Appl Biosaf* 22:52–55. <https://doi.org/10.1177/1535676017713739>.
111. Caporaso JG, Lauber CL, Walters WA, Berg-Lyons D, Lozupone CA, Turnbaugh PJ, Fierer N, Knight R. 2011. Global patterns of 16S rRNA diversity at a depth of millions of sequences per sample. *Proc Natl Acad Sci U S A* 108(Suppl 1):4516–4522. <https://doi.org/10.1073/pnas.1000080107>.
112. Clemente JC, Pehrsson EC, Blaser MJ, Sandhu K, Gao Z, Wang B, Magris M, Hidalgo G, Contreras M, Noya-Alarcón Ó, Lander O, McDonald J, Cox M, Walter J, Oh PL, Ruiz JF, Rodriguez S, Shen N, Song SJ, Metcalf J, Knight R, Dantas G, Dominguez-Bello MG. 2015. The microbiome of uncontacted Amerindians. *Sci Adv* 1:e1500183. <https://doi.org/10.1126/sciadv.1500183>.
113. Dominguez-Bello MG, De Jesus-Laboy KM, Shen N, Cox LM, Amir A, Gonzalez A, Bokulich NA, Song SJ, Hoashi M, Rivera-Vinas JI, Mendez K, Knight R, Clemente JC. 2016. Partial restoration of the microbiota of cesarean-born infants via vaginal microbial transfer. *Nat Med* 22:250–253. <https://doi.org/10.1038/nm.4039>.
114. Bokulich NA, Kaehler BD, Rideout JR, Dillon M, Bolyen E, Knight R, Huttley GA, Gregory Caporaso J. 2018. Optimizing taxonomic classification of marker-gene amplicon sequences with QIIME 2's q2-feature-classifier plugin. *Microbiome* 6:90. <https://doi.org/10.1186/s40168-018-0470-z>.
115. R Core Team. Accessed 28 September 2021. R: a language and environment for statistical computing. <https://www.R-project.org/>.
116. Wickham H. 2016. ggplot2: elegant graphics for data analysis. Springer-Verlag, New York, NY.